Acta Crystallographica Section F
Structural Biology and Crystallization Communications
ISSN 1744-3091

Ardina Grüber, Malathy S. S. Manimekalai, Peter R. Preiser and Gerhard Grüber*

Nanyang Technological University, School of Biological Sciences, 60 Nanyang Drive, Singapore 637551, Singapore

Correspondence e-mail: ggrueber@ntu.edu.sg

Received 31 August 2010
Accepted 12 October 2010

Crystallographic studies of the coupling segment NBD94$_{674–781}$ of the nucleotide-binding domain of the *Plasmodium yoelii* reticulocyte-binding protein Py235

The *Plasmodium yoelii* reticulocyte-binding protein Py235 has a role as an ATP/ADP sensor. The sensor domain of Py235 is called NBD94; it consists of at least three functional regions, the nucleotide-binding region (NBD94$_{444–547}$), hinge region (NBD94$_{566–663}$) and C-terminal coupling region (NBD94$_{674–781}$), and has been proposed to link ATP/ADP binding to the interaction of Py235 with the red blood cell. Here, NBD94$_{674–781}$ was cloned, expressed and purified to high purity. The monodisperse protein was crystallized by vapour diffusion. A diffraction data set was collected to 2.9 Å resolution with 97.2% completeness using a synchrotron-radiation source. The crystals belonged to space group *C*2, with unit-cell parameters a = 65.08, b = 82.71, c = 114.27 Å, β = 94.72°, and contained four molecules in the asymmetric unit.

1. Introduction

Malaria is caused by unicellular protozoan parasites, the life cycle of which in the vertebrate host is characterized by the invasive forms of the sporozoite and merozoite that invade hepatocytes and erythrocytes, respectively (Rodriguez *et al.*, 2008; Gaur *et al.*, 2004). Multiple merozoite protein families have been implicated in the invasion of red blood cells (RBCs), including the reticulocyte-binding protein homologues (RH), which bind to different RBC membrane receptors (Cowman & Crabb, 2006). Little is known about how the large RH transmembrane proteins mediate their function during erythrocyte invasion, but a crucial step appears to be proteolytic cleavage during the invasion process (Triglia *et al.*, 2009). In the malaria parasite *Plasmodium yoelii*, which has been widely studied in order to understand the interaction between the parasite and the host cell (Landau & Gautret, 1998), the RH protein, termed Py235 (235 kDa in mass), has been shown to be a potential virulence factor that allows the parasite to invade a wider range of host erythrocytes (Freeman *et al.*, 1980; Holder & Freeman, 1981). Previously, a 94 kDa domain of Py235 of *P. yoelii* which is highly conserved amongst the RHs has been found to selectively bind ATP and ADP and was termed the nucleotide-binding domain (NBD94; Ramalingam *et al.*, 2008). The

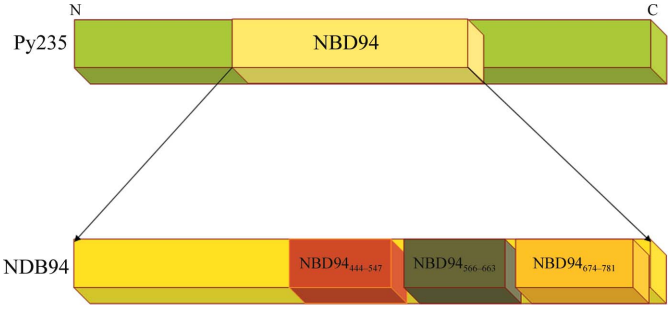

Figure 1
Domain features of Py235 from *P. yoelii*. NBD94 is divided into at least three functional and structural segments: the nucleotide-binding region (NBD94$_{444–547}$), hinge region (NBD94$_{566–663}$) and C-terminal segment (NBD94$_{674–781}$).

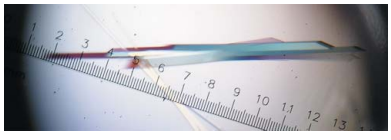

© 2010 International Union of Crystallography
All rights reserved

Table 1
Statistics of crystallographic data collection for NBD94$_{674–781}$.

Values in parentheses are for the highest resolution shell.

Wavelength (Å)	1.000
Space group	*C*2
Unit-cell parameters (Å, °)	*a* = 65.08, *b* = 82.71, *c* = 114.27, β = 94.72
Resolution range (Å)	30–2.90 (3.00–2.90)
No. of unique reflections	13908
Total no. of reflections	27346
Completeness (%)	97.2 (95.2)
R_{merge}† (%)	7.8 (31.1)
Multiplicity	3.0 (2.8)
Mean $I/\sigma(I)$	14.6 (3.6)
Mosaicity (°)	0.8

† $R_{merge} = \sum_{hkl}\sum_i |I_i(hkl) - \langle I(hkl)\rangle| / \sum_{hkl}\sum_i I_i(hkl) \times 100$, where $\langle I(hkl)\rangle$ is the average intensity of reflection *hkl* and $I_i(hkl)$ is the intensity of the *i*th measurement of reflection *hkl*.

preference for MgATP over MgADP recognition is associated with specific structural alterations in the C-terminal domain of NBD94, as depicted by spectroscopic comparison of NBD94 and its C-terminally truncated form NBD94$_{1–550}$, in which no nucleotide-dependent alteration could be observed (Ramalingam *et al.*, 2008). This nucleotide effect in the recombinant protein is potentially significant, as demonstrated by a strong binding of Py235 to red blood cells in the presence of MgATP, which becomes greatly reduced either in the presence of MgADP or in the absence of nucleotides (Ramalingam *et al.*, 2008). Based on these traits and the absence of significant ATPase activity of NBD94, this domain has been suggested to serve as an ATP/ADP sensor during the invasion process (Ramalingam *et al.*, 2008). NBD94 is divided into at least three functional and structural segments, the nucleotide-binding region (NBD94$_{444–547}$), which includes the 8-N_3-3′-biotinyl-ATP-binding sequence, the hinge region (NBD94$_{566–663}$) and the C-terminal segment (NBD94$_{674–781}$), which consists of amino-acid residues 674–781 (Fig. 1). In all hypothetical models described, the sensing of ATP-ADP binding in NBD94$_{444–547}$ by the middle element NBD94$_{566–663}$ is transmitted to NBD94$_{674–781}$, resulting in significant structural rearrangements, thereby facilitating the coupling of nucleotide signalling and Py235 binding to the blood cell. Most recently, the low-resolution solution and crystallographic structure of NBD94$_{444–547}$ and NBD94$_{566–663}$, respectively, have been determined (Grüber *et al.*, 2010). The shape of NBD94$_{444–547}$ in solution was calculated from small-angle X-ray scattering data, revealing an elongated molecule comprised of two globular domains linked by a spiral segment. The crystal structure of the hinge region, including residues 566–663, consists of two helices of 97.8 and 48.6 Å in length linked by a loop (Grüber *et al.*, 2010).

To shed light on the structural basis of the C-terminal coupling element NBD94$_{674–781}$, together with the associated events of ATP/ADP binding and rearrangement of NBD94$_{674–781}$ on Py235 binding to the blood cell, it is necessary to obtain a high-resolution atomic structure of NBD94$_{674–781}$. Here, we describe the cloning, production and crystallization of NBD94$_{674–781}$ from *P. yoelii*.

2. Materials and methods

2.1. Cloning and overexpression

The coding region for NBD94$_{674–781}$ was amplified by PCR using genomic DNA of *P. yoelii* YM. The amplified products, incorporating *Nco*I and *Sac*I restriction sites, were digested and ligated into the 6×His (N-terminal) gene fusion vector pET9-d1 (Grüber *et al.*, 2002). The forward primer 5′-ATA AAG ATC CAT GGT ACA TTA TAT TAC TAG-3′ and the reverse primer 5′-GTT TTC TTT GAG CTC TTA GAT GGT TTT AA-3′ were used to amplify and clone NBD94$_{674–781}$. The plasmid was transformed into *Escherichia coli* strain BL21 (DE3) cells. To express the protein, which consisted of the N-terminal amino-acid sequence HHHHHHPMV followed by the NBD94$_{674–781}$ protein sequence, liquid cultures were grown at 310 K in Luria–Bertani (LB) medium containing kanamycin. To induce protein production, the cultures were supplemented with isopropyl β-D-1-thiogalactopyranoside to a final concentration of 1 m*M*, followed by incubation for a further 4 h at 310 K.

2.2. Protein purification

Bacterial cells containing recombinant NBD94$_{674–781}$ protein were harvested from 2 l cultures by centrifugation at 8000*g* for 10 min at 279 K. The cells were lysed on ice in 50 ml buffer *A* (50 m*M* Tris–HCl pH 7.5, 200 m*M* NaCl and 2 m*M* PMSF) by sonication with an Ultrasonic Homogenizer (Bandelin, Tip KE76) for 3 × 1 min. After sonication, the cell lysate was centrifuged at 10 000*g* for 35 min at 277 K. The resulting supernatant was passed through a filter (0.45 µm pore size) and supplemented with 2 ml Ni–NTA resin pre-equilibrated in buffer *A*. The His-tagged protein was allowed to bind to the matrix for 1 h at 277 K by mixing on a sample rotator (Neolab). Ni–NTA resin with bound 6×His-tagged protein was poured into a column and washed using 8 ml buffer *A* without imidazole. Protein was eluted with an imidazole gradient (0–250 m*M*) in buffer *A* by gravity-flow chromatography. Fractions containing the required protein were identified by SDS–PAGE (Laemmli, 1970), pooled and concentrated using a Millipore spin concentrator with a molecular-mass cutoff of 10 kDa. The sample was applied onto a Superdex HR75 (10/30, GE Healthcare) gel-filtration column using 50 m*M* Tris–HCl pH 7.5, 200 m*M* NaCl, 2 m*M* PMSF and 10 m*M* EDTA and a flow rate of 0.5 ml min^{-1}. Respective fractions were concentrated in Millipore spin concentrators. The purity of the protein sample was analyzed by SDS–PAGE (Laemmli, 1970) stained with Coomassie Brilliant Blue R250.

2.3. Circular-dichroism (CD) spectroscopy

Steady-state CD spectra were measured in the far UV (190–260 nm) using a Chirascan spectropolarimeter (Applied Photophysics). Spectra were collected using a 60 µl quartz cell (Hellma) with a path length of 0.1 mm at 293 K and a step resolution of 1 nm. The readings were for an average of 2 s at each wavelength and the recorded ellipticity values were the average of three determinations for each sample. CD spectroscopy of recombinant NBD94$_{674–781}$ (2.0 mg ml^{-1}) was performed in a buffer consisting of 50 m*M* Tris–HCl pH 7.5 and 200 m*M* NaCl. The buffer spectrum was subtracted from the protein spectrum. CD values were converted to mean residue ellipticity (Θ) in units of deg cm^2 dmol^{-1} using the software *Chirascan* v.1.2 (Applied Photophysics). This baseline-corrected spectrum was used as input for computer methods to obtain predictions of secondary structure. In order to analyze the CD spectrum, the following algorithms were used: *Varselec* (Manavalan & Johnson, 1987), *Selcon* (Sreerama & Woody, 1993), *CONTIN* (Provencher, 1982), *K2D* (Andrade *et al.*, 1993) (all methods as incorporated into the program *DICROPROT*; Deléage & Geourjon, 1993) and *CDNN* (Bohm *et al.*, 1992). The normalized root-mean-square deviation (NRMSD) was calculated according to Whitmore & Wallace (2004).

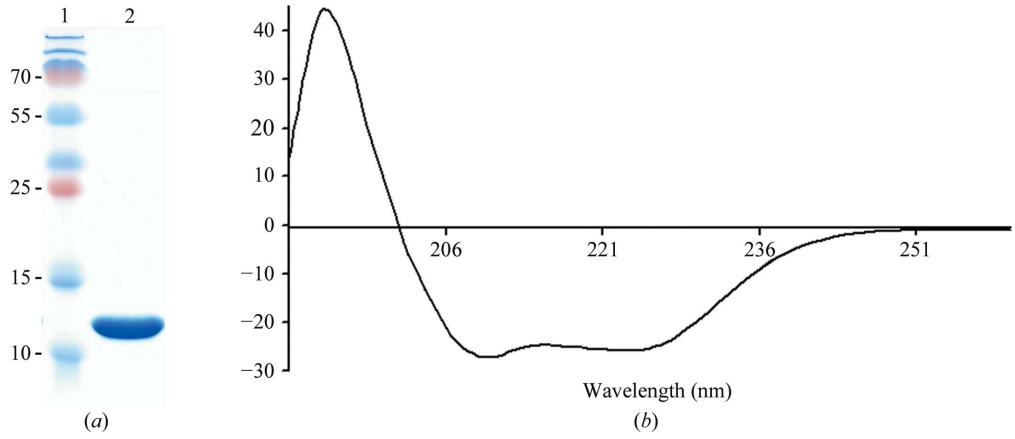

Figure 2
(*a*) SDS gel (17% total acrylamide and 0.4% cross-linked acrylamide) of purified recombinant NBD94$_{674–781}$ from *P. yoelii*; lane 1 contains protein markers (labelled in kDa). (*b*) Far-UV CD spectrum of NBD94$_{674–781}$ (2 mg ml^{-1}).

2.4. Crystallization conditions

The purified protein was concentrated to 13 mg ml^{-1} in 50 m*M* Tris pH 7.5, 200 m*M* NaCl using a 10 kDa cutoff concentrator. Preliminary screening for initial crystallization conditions was performed by the hanging-drop vapour-diffusion method using screens from Hampton Research at 296 K by mixing 1 µl droplets of concentrated protein solution with an equal volume of reservoir solution and equilibrating over 500 µl reservoir solution using 24-well Cryschem plates (Hampton Research, USA).

2.5. X-ray data collection and analysis

The crystal was quick-soaked in a cryoprotectant solution containing Paratone and mineral oil in a 1:1 ratio and flash-cooled in liquid nitrogen at 100 K. Single-wavelength data sets were collected for NBD94$_{674–781}$ crystals at 140 K on beamline 13B1 at the National Synchrotron Radiation Research Center (NSRRC, Hsinchu, Taiwan) using an ADSC Quantum 315 CCD detector. The diffraction data were indexed, integrated and scaled using the *HKL*-2000 suite of programs (Otwinowski & Minor, 1997). Data-collection statistics are given in Table 1.

3. Results and discussion

3.1. Protein characterization

SDS–PAGE of recombinant NBD94$_{674–781}$ revealed a prominent band of about 14 kDa found entirely within the soluble fraction, which was purified by affinity and size-exclusion chromatography (Fig. 2*a*). The secondary structure of this protein was determined from the circular-dichroism spectrum (Fig. 2*b*). The CD spectrum of NBD94$_{674–781}$ shows that the protein is mainly α-helical, as reflected by its minima at 208 and 222 nm and as predicted from its amino-acid sequence. The α-helical content of NBD94$_{674–781}$ was determined to be 70%. This result is consistent with secondary-structure predictions based on the amino-acid sequence of NBD94$_{674–781}$, revealing an α-helical content of 71% and reflecting the correct secondary structure of the generated recombinant protein. The normalized root-mean-square deviation (NRMSD) of the experimental and calculated spectra was 0.06. The molar ellipticity values at 208 and 222 nm of NBD94$_{674–781}$ are in a ratio of 0.97, indicating that many of the residues in NBD94$_{674–781}$ are in close proximity; non-interacting helices typically give ratios of around 0.8.

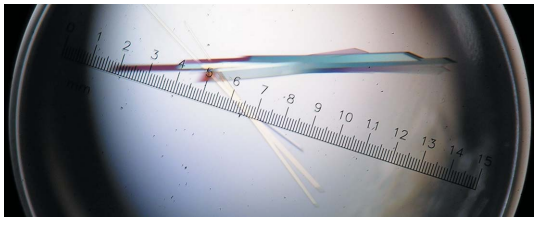

Figure 3
Crystals of NBD94$_{674–781}$ from *P. yoelii*. The crystals are approximately 0.3 × 0.4 × 1.4 mm in size.

3.2. Crystallization and preliminary X-ray analysis

Crystals of good diffraction quality appeared in about 4 d from an optimized condition consisting of 0.1 *M* citric acid pH 5.0, 10%(*w*/*v*) PEG 6000 from Hampton Research Grid Screen PEG 6000 and were further optimized by systematically adjusting the protein and buffer concentrations. Finally, optimized native crystals were grown at 10 mg ml^{-1} protein concentration in 0.1 *M* citric acid pH 5.0, 10%(*w*/*v*) PEG 6000. A typical crystal is shown in Fig. 3 with dimensions of 0.3 × 0.4 × 1.4 mm. Analysis of the crystal by SDS–PAGE and MALDI mass spectrometry revealed the molecular mass to be 12.6 kDa, indicating that the entire protein is present in the crystal.

These crystals diffracted to 2.9 Å resolution and belonged to space group *C*2, with unit-cell parameters a = 65.08, b = 82.71, c = 114.27 Å, β = 94.72°. Assuming the presence of four molecules in the asymmetric unit, the solvent content is 55.81% and V_M is 2.78 Å^3 Da^{-1} (Matthews, 1968). However, at this stage we cannot rule out the possibility of five (solvent content 44.77%, V_M = 2.23 Å^3 Da^{-1}) or six (solvent content 33.72%, V_M = 1.85 Å^3 Da^{-1}) molecules in the asymmetric unit, which will be clarified when the structure is solved. Research is in progress to determine the three-dimensional structure of the coupling segment NBD94$_{674–781}$.

We thank the staff of beamline 13B1 at the National Synchrotron Radiation Research Centre (NSRRC), a national user facility supported by the National Science Council of Taiwan, ROC, and Dr Asha M. Balakrishna (SBS, NTU) for expert help with data collection. The Synchrotron Radiation Protein Crystallography Facility at NSRRC is supported by the National Research Program for

Genomic Medicine. This research was supported by A*STAR BMRC (08/1/22/19/613).

References

Andrade, M. A., Chacon, P., Merelo, J. J. & Moran, F. (1993). *Protein Eng. Des. Sel.* **6**, 383–390.

Bohm, G., Muhr, R. & Jaenicke, R. (1992). *Protein Eng. Des. Sel.* **5**, 191–195.

Cowman, A. F. & Crabb, B. S. (2006). *Cell*, **124**, 755–766.

Deléage, G. & Geourjon, C. (1993). *Comput. Appl. Biosci.* **9**, 197–199.

Freeman, R. R., Trejdosiewicz, A. J. & Cross, G. A. (1980). *Nature (London)*, **284**, 366–368.

Gaur, D., Mayer, D. C. & Miller, L. H. (2004). *Int. J. Parasitol*. **34**, 1413–1429.

Grüber, A., Manimekalai, M. S. S., Balakrishna, A., Hunke, C., Jeyakanthan, J., Preiser, R. P. & Grüber, G. (2010). *PLoS ONE*, **5**, e9146.

Grüber, G., Godovac-Zimmermann, J., Link, T. A., Coskun, Ü., Rizzo, V. F., Betz, C. & Bailer, S. M. (2002). *Biochem. Biophys. Res. Commun.* **298**, 383–391.

Holder, A. A. & Freeman, R. R. (1981). *Nature (London)*, **294**, 361–364.

Laemmli, U. (1970). *Nature (London)*, **227**, 680–685.

Landau, I. & Gautret, P. (1998). *Malaria: Parasite Biology, Pathogenesis and Protection*, edited by I. W. Sherman, pp. 401–417. Washington DC: American Society for Microbiology.

Manavalan, P. & Johnson, W. C. Jr (1987). *Anal. Biochem.* **167**, 76–85.

Matthews, B. W. (1968). *J. Mol. Biol.* **33**, 491–497.

Otwinowski, Z. & Minor, W. (1997). *Methods Enzymol.* **276**, 307–326.

Provencher, S. W. (1982). *Comput. Phys. Commun.* **27**, 213–227.

Ramalingam, K. J., Hunke, C., Gao, X., Grüber, G. & Preiser, R. P. (2008). *J. Biol. Chem.* **283**, 36389–36396.

Rodriguez, L. E., Curtidor, H., Uriquiza, M., Cifuentes, G., Reyes, C. & Patarroyo, M. E. (2008). *Chem. Rev.* **108**, 3656–3705.

Sreerama, N. & Woody, R. W. (1993). *Anal. Biochem.* **209**, 32–44.

Triglia, T., Tham, W. H., Hodder, A. & Cowman, A. F. (2009). *Cell. Microbiol.* **11**, 1671–1687.

Whitmore, L. & Wallace, B. A. (2004). *Nucleic Acids Res.* **32**, W668–W763.